European Journal of Pharmaceutics and Biopharmaceutics 72 (2009) 358–369

Contents lists available at ScienceDirect

European Journal of Pharmaceutics and Biopharmaceutics

journal homepage: www.elsevier.com/locate/ejpb

Research paper

The influence of chitosan content in cationic chitosan/PLGA nanoparticles on the delivery efficiency of antisense 2′-*O*-methyl-RNA directed against telomerase in lung cancer cells

S. Taetz [a], N. Nafee [a], J. Beisner [b], K. Piotrowska [b], C. Baldes [a], T.E. Mürdter [b], H. Huwer [c], M. Schneider [d], U.F. Schaefer [a], U. Klotz [b], C.-M. Lehr [a,*]

[a] *Biopharmaceutics and Pharmaceutical Technology, Saarland University, Saarbrücken, Germany*
[b] *Dr. Margarete Fischer–Bosch Institute of Clinical Pharmacology and University of Tübingen, Stuttgart, Germany*
[c] *SHG Kliniken Völklingen, Center for Heat and Thorax Surgery, Völklingen, Germany*
[d] *Pharmaceutical Nanotechnology, Saarland University, Saarbrücken, Germany*

ARTICLE INFO

Article history:
Received 15 May 2008
Accepted in revised form 8 July 2008
Available online 27 July 2008

Keywords:
Chitosan PLGA nanoparticles
Antisense 2′-*O*-methyl-RNA
Telomerase
Lung cancer
A549
Calu-3
Primary human alveolar epithelial cells

ABSTRACT

Tailorable cationic chitosan/PLGA nanoparticles (CPNP) were used for the delivery of an antisense 2′-*O*-methyl-RNA (2OMR) directed against RNA template of human telomerase. Here, we describe the influence of the chitosan content on binding efficiency, complex stability, uptake in different human lung cell types and finally demonstrate the efficacy of this nanoplex system.

CPNPs were prepared by the emulsion-solvent evaporation method using different amounts of chitosan and purified by preparative size exclusion chromatography. The characterization by photon correlation spectroscopy and zeta potential measurements showed a small increase in size and an increase of zeta potential with increasing amounts of chitosan. Binding efficiency and complex stability with 2OMR was high in water and correlated well with the chitosan content of particles but was weak in physiologically relevant media (PBS and RPMI cell culture medium). However, flow cytometry analysis showed that the uptake of 2OMR into A549 lung cancer cells was considerably higher in combination with nanoparticles and dependent on the amount of chitosan when compared to 2OMR alone. Confocal laser scanning microscopy revealed that the uptake into A549 cells is mediated via complexes of 2OMR and chitosan/PLGA nanoparticles despite the weak binding in cell culture medium. The nanoparticles were well tolerated and efficient in inhibiting telomerase activity.

1. Introduction

The treatment of genetic disorders by the administration of exogenous plasmid DNA or the inhibition of gene expression by antisense oligonucleotides or siRNA are promising approaches for the treatment of severe diseases like cancer in the future. However, it is a well-recognized fact that the main obstacle for gene therapy or the therapeutical application of antisense oligonucleotides and siRNA is the lack of a safe and efficient delivery strategy for nucleotide-based drugs *in vivo*.

Our studies focus on the treatment of non-small cell lung cancer by telomerase inhibition. Telomerase is a ribonucleoprotein with reverse transcriptase activity that plays an important role in cell immortalization and cancer development by maintaining chromosomal ends, the telomeres. Telomeres are non-coding, repetitive hexameric $(TTAGGG)_n$ sequences that form lasso-like structures. They are important for chromosomal protection and the control of cell proliferation. In normal cells telomeres shorten during each cell cycle due to the end-replication problem. When they reach a certain limit it is a signal for the cell to stop dividing and enter the state of cellular senescence. Further cell divisions would result in non-functional telomeres and severe chromosomal damages. Cells that express the enzyme telomerase, like most cancer cells, escape this mechanism and can divide indefinitely. Therefore, the reintroduction of the normal cell cycle by telomerase inhibition is an interesting strategy for cancer treatment [1,2].

A search for suitable telomerase inhibitors resulted in an antisense 2′-*O*-methyl-RNA (2OMR) [3] directed against the template region of human telomerase RNA (hTR) that has been reported to

Abbreviations: 2OMR, 2′-*O*-methyl RNA; CLSM, confocal laser scanning microscopy; CPNP, chitosan/PLGA nanoparticels; FAM, carboxyfluorescein; FCS, fetal calf serum; hAEpC, human alveolar epithelial cells; PBS, phosphate buffered saline; PdI, polydispersity index; PLGA-NP, poly(lactic-co-glycolic acid) nanoparticles; TEER, transepithelial electrical resistance; ZP, zeta potential.

* Corresponding author. Biopharmaceutics and Pharmaceutical Technology, Saarland University, P.O. Box 15 11 50, 66041 Saarbrücken, Germany. Tel.: +49 681 302 3039; fax: + 49 681 302 4677.
E-mail address: lehr@mx.uni-saarland.de (C.-M. Lehr).

0939-6411/$ - see front matter © 2009 Published by Elsevier B.V.
doi:10.1016/j.ejpb.2008.07.011

be a highly potent and sequence-selective inhibitor of human telomerase [4,5]. Our group previously developed chitosan-coated poly(lactic-co-glycolic acid) (PLGA) nanoparticles based on an emulsion – diffusion – solvent-evaporation method. These nanoparticles proved to be efficient carriers for the delivery of plasmid DNA into A549 lung cancer cells *in vitro* and lungs of mice after intranasal administration *in vivo* [6,7]. The advantage of these nanoparticles is that their properties with respect to size and surface charge can easily be modified in a controlled manner by varying the amounts of PLGA, chitosan and PVA during particle preparation [8]. However, although plasmid DNA and antisense oligonucleotides might be regarded to be similar from the chemical point of view their differences in size are likely to influence the properties of complexes formed with nanoparticles and hence their biological efficacy. Therefore, a re-evaluation of these chitosan/PLGA nanoparticles as a carrier system for antisense 2OMR was necessary. The aim of the present study was to evaluate the nanoparticles with regard to binding efficiency, complex stability of nanoplexes in biologically relevant media, their delivery efficacy of the telomerase inhibitor to lung cancer cells and the inhibition of telomerase activity.

2. Materials and methods

2.1. Materials

Poly(lactic-co-glycolic acid) (PLGA) 70:30 was purchased from Polysciences Europe GmbH (Eppelheim, Germany), polyvinylalcohol (PVA) Mowiol® 4–88 from Kuraray Specialities Europe GmbH (Frankfurt, Germany), ultrapure chitosan chloride Protasan™ UP CL113 with a molecular weight of 50–150 kDa and a degree of deacetylation between 75% and 90% from NovaMatrix (FMC BioPolymer, Drammen, Norway) and ethyl acetate from Fluka Chemie GmbH (Buchs, Switzerland).

Antisense oligonucleotide 2′-*O*-methyl-RNA (2OMR) with a phosphorothioate (ps) backbone (5′-2′-*O*-methyl [C(ps)A(ps)-GUUAGGGUU(ps)A(ps)G]-3′) directed against human telomerase RNA (hTR), its carboxyfluoresceinamine labeled derivative 5′-FAM-2OMR and a mismatch sequence (5′-2′-*O*-methyl [C(ps)A(ps)-GUUAGAAUU(ps)A(ps)G]-3′) were obtained from Biomers.net GmbH (Ulm, Germany).

2.2. Nanoparticle preparation

Chitosan-coated PLGA nanoparticles were prepared by an emulsion-diffusion-evaporation technique as described by Kumar et al. [6] and Nafee et al. [8]. In brief, 5 ml of PLGA dissolved in ethyl acetate (20 mg/ml) were added dropwise to 5 ml of an aqueous chitosan solution containing 2.5% w/v PVA under magnetic stirring. The emulsion was stirred at 1000 rpm for 1 h. Afterwards, it was homogenized using an UltraTurrax T25 (Janke & Kunkel GmbH & Co-KG, Germany) at 13,500 rpm for 15 min. The homogenized emulsion was diluted to a volume of 50 ml under constant stirring with MilliQ-water. Remaining ethyl acetate was evaporated by continuous stirring over night at room temperature. The concentrations of chitosan in the aqueous phase were varied to obtain nanoparticles with different surface charges as has been shown by Nafee et al. [8] 0 mg/ml (pure PLGA nanoparticles; PLGA-NP), 0.5 mg/ml (05CPNP), 1 mg/ml (1CPNP), 3 mg/ml (3CPNP) and 6 mg/ml (6CPNP). The abbreviations in parentheses will be used throughout the document as reference to the different particle preparations. CPNP stands for *c*hitosan-coated *P*LGA *n*ano*p*articles.

Red fluorescently labeled chitosan/PLGA nanoparticles were prepared as described above but with 2 μM of the lipophilic dye DiI (1,1′-dioctadecyl-3,3,3′,3′-tetramethylindocarbocyanine perchlorate; from Sigma–Aldrich Chemie GmbH, Taufkirchen, Germany) in the organic phase. The chitosan concentration for this preparation in the aqueous phase was 3 mg/ml (DiICPNP).

2.3. Purification of nanoparticles

Chitosan/PLGA nanoparticles were purified from excess PVA by preparative size exclusion chromatography (SEC) using an FPLC® system from Pharmacia Biotech (now Amersham Biosciences; Uppsala, Sweden) equipped with two P-500 pumps, a LCC-501 Plus controller, a MV-7 injection valve, a 50 ml Superloop, a C 16/70 column with one AC 16 adaptor, an Uvicord SII detector with an interference filter of 206 nm and a FRAC-100 fraction collector. Stationary phase was Sephacryl 1000-SF® from GE Healthcare (Munich, Germany) with a dimension of 65 cm in height and 1.6 cm in diameter. Mobile phase was degassed MilliQ-water containing 0.1 mM HCl. The system was operated by the FPLCdirector™ version 1.3 (Pharmacia Biotech).

Nanoparticles were filtered through non-sterile a 0.2 μm cellulose acetate filter (Chromafil® GF/PET-20/25, Macherey-Nagel, Düren, Germany) prior to purification to prevent clogging of the stationary phase. Injection volumes were 5–7 ml per run. Flow rate of mobile phase was 1 ml/min under isocratic conditions. Purified particles were collected and concentrated by ultrafiltration using Vivaspin 20® (Sartorius, Göttingen, Germany) with a molecular weight cut-off of 300,000 Da at 1000 ×*g*. Afterwards they were sterile filtered (0.2 μm, Minisart® sterile cellulose acetate filter, Sartorius). Concentrations of nanoparticles were determined gravimetrically after lyophilization. PVA from pure PLGA nanoparticle suspension was removed by five centrifugation/ resuspension (with MilliQ-water) cycles in Vivaspin 20® because it was not possible to purify the pure PLGA nanoparticles by the size exclusion method described above. Purified and sterile filtered particle suspensions were stored at 4 °C.

2.4. Characterization of nanoparticle properties

Particle characteristics were determined directly after preparation, after purification, concentration and filtration and after a storage period of about two months at 4 °C. They were characterized with respect to size, polydispersity index (PdI) and surface charge. Size and PdI were determined by photon correlation spectroscopy and surface charge by measuring the zeta potential in a ZetaSizer Nano ZS from Malvern Instruments Ltd. (Worcestershire, UK). The ZetaSizer was equipped with a 4 mW He–Ne laser. Measurements were performed at 633 nm and a backscattering angle of 173°. Samples were diluted in MilliQ-water. All measurements were performed in triplicate at 25 °C using the standard settings for water as dispersion medium.

2.5. Formation of 2OMR-chitosan/PLGA nanoplexes

Complexation experiments were performed in MilliQ-water, phosphate buffered saline (PBS) pH 7.4 and RPMI cell culture medium (without phenol red; PAA Laboratories GmbH, Pasching, Austria) containing 10% fetal calf serum (FCS; Sigma–Aldrich). For this purpose a fixed amount of 2′-*O*-methyl-RNA (2OMR) was mixed and incubated with different amounts of purified chitosan/PLGA nanoparticles. The concentration of oligonucleotides was 4 μM which corresponds to 17.72 μg/ml for non-labeled 2OMR and 19.84 μg/ml for 5′-FAM-2OMR, respectively.

For complex formation 100 μl of a 5-fold concentrated oligonucleotide solution in MilliQ-water was mixed with particles at the following weight:weight ratios (concentrations in parentheses refer to the final concentrations of particles in the suspensions): 1:0 (=100% unbound oligonucleotides), 1:1 (17.72 μg/ml particles),

1:5 (88.6 μg/ml particles), 1:10 (177.2 μg/ml particles), 1:25 (443 μg/ml particles), 1:50 (886 μg/ml particles) and 1:100 (1772 μg/ml particles). The mixtures were vortexed thoroughly and incubated at room temperature for about 10 min. Afterwards the volume was made up to 500 μl with MilliQ-water, PBS buffer or RPMI cell culture medium (without phenol red) supplemented with 10% FCS, respectively, vortexed again and incubated at room temperature for another 15 min.

After incubation the nanoplex suspensions were centrifuged at about 23,000 × *g* and 25 °C for one hour. Samples from the supernatant were analyzed for unbound oligonucleotide. 2OMR was determined by HPLC analysis. 5′-FAM-2OMR in cell culture medium was quantified by fluorimetry. All experiments were performed in triplicate.

2.6. HPLC analysis of 2′-O-methyl RNA

2′-*O*-methyl RNA (2OMR) from complexation experiments was quantified by reversed phase HPLC using an gradient Dionex HPLC system consisting of an ASI 100 automated sample injector, UVD 170S detector and P580 gradient pump with Chromeleon® software (version 6.50 SP5 build 1023) (Dionex, Idstein, Germany).

The column was a Gemini® RP-18 column (150 × 4.6 mm/5 μm/110 Å) from Phenomenex (Aschaffenburg, Germany). Mobile phase A was composed of 10 mM triethylammonium acetate buffer pH 7.0, mobile phase B was pure acetonitrile. The gradient was as follows: 0–0.3 min: 100% A; 0.3–3.3 min: 100% A–80% A, 20% B; 3.3–6.0 min: 80% A, 20% B; 6.0–9.0 min: 80% A, 20% B–100% A; 9.0–17.0 min: 100% A. Column temperature was 40 °C and the UV detector was set to 260 nm. Injection volume was 50 μl per sample. At a flow rate of 1 ml/min the retention time of 2OMR was 6.47 ± 0.04 min. Detection and quantification limits were 0.025 and 0.050 μg/ml, respectively. Standards were in the linear range of 0.05–20 μg/ml.

2.7. Quantification of 5′-FAM-2′-O-methyl RNA

5′-FAM-labeled 2OMR was quantified by fluorimetry using a Cytofluor II fluorescence reader with Cytofluor software version 4.2 (PerSeptive Biosystems, Wiesbaden-Norderstedt, Germany). 150 μl samples from the supernatant were transferred into a 96-well plate and directly measured. The excitation wavelength was set to 485/20 nm and the emission wavelength to 530/30 nm. Standards were in the linear range of 0.5–20 μg/ml.

2.8. Cell cultures

A549 (CCL-185; ATCC, Manassas, VA, USA) were cultivated in RPMI with L-glutamine (PAA Laboratories GmbH, Pasching, Austria) supplemented with 10% fetal calf serum.

Calu-3 cells (HTB-55; ATCC) were cultivated in Minimum Essential Medium (MEM) with Earl's Salts and L-glutamine (PAA Laboratories GmbH) supplemented with 10% FCS, 1% MEM non-essential amino acid (NEAA) solution and 1 mM sodium pyruvate (all from Sigma–Aldrich).

Primary human alveolar epithelial cells (hAEpC) were isolated from non-tumor lung tissue of patients undergoing partial lung resection according to Elbert et al. [9] with slight modifications of the enzymatic digestion and cell purification [10]. In brief, the chopped tissue was digested using a combination of 150 mg trypsin type I (Sigma) and 3 mg elastase (Worthington Biochemical Corp., Lakewood, NJ, USA) in 30 ml BSS (137.0 mM NaCl, 5.0 mM KCl, 0.7 mM $Na_2HPO_4 \times 7H_2O$, 1.2 mM $MgSO_4 \times 7H_2O$, 5.5 mM Glucose, 10.0 mM HEPES, 0.18 mM $CaCl_2$, 100 U/ml penicillin and 100 μg/ml streptomycin) for 40 min at 37 °C. The alveolar type II (AT II) cell population was purified by a combination of differential cell attachment, percoll density gradient centrifugation and positive selection of epithelial cells with magnetic beads (human Anti-human epithelial antigen (epithelial cells adhesion molecule; Ep-CAM) MicroBeads, Miltenyi Biotec, Bergisch Gladbach, Germany). Cell viability was assessed by trypan blue staining. They were grown in small airway growth medium (SAGM) (Cambrex BioScience Walkersville Inc., Walkersville, MD, USA) supplemented with 1% FCS, 100 units/ml penicillin and 100 μg/ml streptomycin (Sigma–Aldrich). The use of the human material for isolation of primary cells was reviewed and approved by the Ethics Committee of the State Medical Board of Registration of the Saarland.

All cells were kept in an incubator set to 37 °C, 5% CO_2 and 95% humidity.

2.9. Assessment of 2OMR association with cells by flow cytometry

The association of 5′-FAM-labeled 2OMR with A549 cells was studied by flow cytometry by measuring the green fluorescence of the oligonucleotides after incubation with nanoplexes. A549 cells were seeded in 6-well plates at a density of 25,000 cells per well and grown for 3 days. Nanoplexes of 5′-FAM-2OMR and different chitosan/PLGA nanoparticles were prepared at ratios of 1:50 ($w_{2OMR}/w_{particles}$) by incubating the different particle suspensions with oligonucleotides at room temperature for 15 min. Afterwards the nanoplex suspensions were diluted with RPMI cell culture medium containing 10% FCS to the desired final concentration of 4 μM 5′-FAM-2OMR. The cells were incubated with these suspensions for 6 h in the incubator. Subsequently, the incubation medium was exchanged for normal cell culture medium without nanoplexes. Controls were non-treated cells, cells treated with 4 μM 5′-FAM-2OMR alone and cells treated with particle suspensions without 5′-FAM-2OMR. Analysis by flow cytometry was performed the next day with a FACSCalibur flow cytometer from Becton Dickinson (BD) Biosciences (Heidelberg, Germany) using the software CellQuest™ Pro Version 4.02 (BD Biosciences). For this purpose cells were detached by incubation with trypsin/EDTA, washed with PBS and resuspended in sheath fluid (BD Biosciences). Green fluorescence was excited at 488 nm and measured after passing a 530/30 nm band pass filter. The instrument was adjusted with non-treated cells. During each run 20,000 cells were counted. The extent of cell associated 5′-FAM-2OMR was evaluated after gating and selection of a fluorescence threshold referred to non-treated cells. The experiment was performed in triplicate.

2.10. Visualization of cellular uptake by confocal laser scanning microscopy

2.10.1. Preparation of cells

Cells were grown in 16 well LabTek chamber slides (Nunc GmbH, Wiesbaden, Germany; growth area: 0.4 cm^2). A549 cells were seeded at a density of 2500 cells per well 3 days prior to the experiment. Calu-3 cells were seeded at a density of 20,000 cells per well 6 days prior to the experiment. hAEpC were seeded in collagen/fibronectin coated wells at a density of 10,000 cells per well 7 days prior to the experiment. All cells were kept under the conditions described above.

For uptake experiments cells were treated with nanoplexes prepared of 5′-FAM-2OMR and 3CPNP at a w/w ratio of 1:50. Nanoplexes were prepared by mixing and incubating 5′-FAM-2OMR solution and 3CPNP suspension for 15 min at room temperature. The nanoplex suspension was diluted to 4 μM 5′-FAM-2OMR with RPMI cell culture medium containing 10% FCS. Cells were incubated with this medium for 6 h in the incubator. Afterwards the incubation medium was replaced by normal cell culture medium without nanoplexes. If necessary, cell culture medium was exchanged every other day.

2.10.2. Staining of cell membranes and nuclei

Cell membranes were stained with the red fluorescent rhodamine-labeled ricinus communis agglutinin I (Rho-RRCA; excitation maximum 552 nm, emission maximum 577 nm; Vector Laboratories Peterborough, UK). Cells were washed once with PBS and afterwards incubated with 25 μg/ml of Rho-RRCA in PBS for 15 min in the incubator. After two washing steps with PBS the cells were fixed with 4% paraformaldehyde in PBS for 10 min at room temperature.

Cell nuclei were stained with TOPRO-3 (excitation maximum 642 nm, emission maximum 661 nm; Molecular Probes, Invitrogen GmbH, Karlsruhe, Germany). For this purpose the cells were washed once with PBS. Afterwards they were fixed and permeabilized with ice-cold (−20 °C) pure ethanol for 10 min at 4 °C. After two washing steps with PBS the cells were incubated with 1 μM TOPRO3 in PBS for 15 min at room temperature.

After fixation and staining the cells were washed again twice with PBS and were subsequently mounted in the fluorophor protector FluorSafe® reagent (Calbiochem, San Diego, CA, USA) and studied by confocal laser scanning microscopy.

2.10.3. Image acquisition and processing

Confocal laser scanning microscopy was performed with a Bio-Rad 1024 MRC system (Bio-Rad, München, Germany) in combination with an inverted Zeiss Axiovert 100 microscope (Carl Zeiss MicroImaging GmbH, Göttingen, Germany) equipped with a krypton/argon laser and a 40× oil immersion objective (NA 1.3). Excitation wavelengths and emission filter sets were dependent on the staining method and are summarized in Table 1.

A step motor was used for the acquisition of 3D images. Images were processed using the software Volocity® (Improvision, Tübingen, Germany). XY-images in Figs. 4 and 5 are presented in "extended focus" mode, i.e. an overlay of all images in an image stack merged into one image for better presentation. XZ- and YZ-cross sections from the image stacks were used to verify the localization of the green fluorescence of 5′-FAM-2OMR with respect to the stained membrane.

2.11. Cytotoxicity experiments and monolayer integrity

Cytotoxicity of 3CPNP was determined by the MTT [(3-(4,5-dimethylthiazol-2-yl)-2,5-diphenyltetrazolium bromide] assay. A549 cells were seeded on 96-well plates at a density of 10,000 cells per well and were allowed to adhere overnight. The next day cells were incubated for 6 hours with 3CPNP and nanoplexes of 2OMR and 3CPNP in cell culture medium at particle concentrations of 443, 886 and 1772 μg/ml. The corresponding nanoplex ratios were 1:25, 1:50 and 1:100 (w_{2OMR}/w_{3CPNP} ratios; where 1 = 17.72 μg/ml = 4 μM 2OMR final concentration). Cells treated with cell culture medium and cell culture medium diluted with water (at a volume corresponding to the highest CPNP concentration) were included for comparison. After incubation the medium was exchanged for normal cell culture medium and the cells were grown for three more days. On the third day 10 μl of 10 mg/ml MTT solution in PBS pH 7.4 were added to each well. After an incubation time of 2 hours under cell culture conditions 90 μl lysis buffer (15% SDS in a 1:1 mixture of dimethylformamide and water, pH adjusted to 4.5 with 80% acetic acid) were added to each well. Cell lysis was performed at room temperature overnight on an orbital shaker. Absorbance was measured the next day at 560 nm. Each concentration was measured in quadruplicate.

The influence of chitosan/PLGA nanoparticles on the integrity of cell monolayers was assessed by measuring the transepithelial electrical resistance (TEER) using an epithelial voltohmmeter (EVOM, World Precision Instruments, Berlin, Germany) with an STX-2 electrode. Calu-3 cells were grown on 12 mm polyester (PET) Transwell® filters (Corning Inc., NY, USA) at a density of 100,000 cells per filter for 3 weeks. Cells were treated with 0.5, 1 and 2 mg/ml of purified 3CPNP in cell culture medium containing 10% FCS. Control cells were treated with cell culture medium only and a 1:1 mixture of cell culture medium with sterile MilliQ-water, respectively. The mixture with water was used to check for the influence in changes of osmotic pressure that might occur upon dilution of cell culture medium. Cells were incubated for 6 h. Afterwards the incubation medium was replaced by normal cell culture medium. TEER values were measured before incubation, after 3 and 6 h and after 3 days of incubation. Measurements were performed in hexaplicate.

Table 1
Excitation wavelengths and filters for confocal microscopy depending on the staining method

Staining method	Excitation wavelength (nm)	Emission filter
Two colors (dyes)		
Green (5′-FAM-2OMR)	488	522/35 nm BP
Red (Rho-RRCA)	568	585 nm LP
Three colors		
Green (5′-FAM-2OMR)	488	522/35 nm BP
Red (DiI)	568	605/32 nm BP
Far red (TOPRO-3)	647	680/32 nm BP

BP, band pass filter; LP, long pass filter.

2.12. Telomerase activity measurement (TRAP)

Cells (1×10^6) were collected and lysed in 200 μL ice-cold CHAPS lysis buffer (10 mM Tris–HCl (pH 7.5), 1 mM $MgCl_2$, 1 mM EGTA, 0.1 mM Benzamidine, 5 mM β-mercaptoethanol, 0.5% CHAPS (3-[(3-cholamidopropyl)dimethyl-ammonio]-1-propanesulfonate), 10% glycerol) for 30 min on ice. Lysates were centrifuged at 12,000g for 20 min at 4 °C and the supernatants were snap-frozen and stored at −80 °C. Telomerase activity was measured in lysates containing 0.05 μg protein using a modified protocol of the TRA-Peze Telomerase detection kit. The manufacturer's protocol was modified as follows: A 6-carboxy-fluorescein (6-FAM) labeled TS primer 5′-AATCCGTCGAGCAGAGTT-3′ and CX primer 5′-CCCTTACCCTT-ACCCTTACCCTAA-3′ were used. An internal telomerase assay standard (ITAS) which represents a 150 bp fragment of the rat myogenin cDNA which is amplified by TS and CX primer was added in the reaction mix. PCR products were separated by fluorescence capillary electrophoresis (ABI PRISM 310 Genetic Analyzer). Fragment sizes were determined using the internal size standard GeneScan-500 ROX and collected data were analyzed with GeneScan Analysis software.

2.13. Terminal restriction fragment length determination (TRF)

DNA was isolated from cells using the phenol/chloroform extraction method, digested with 10 U of Hinf I, electrophoresed and transferred to a nylon membrane. The nylon membrane was hybridized with a digoxigenin labeled 5′-$(TTAGGG)_7$ telomere-specific probe and incubated with anti-DIG-alkaline phosphatase. The immobilized telomere probe was visualized by a chemiluminescent substrate for alkaline phosphatase (CDP-star, Roche). The membrane was exposed to X-ray film (Hyperfilm; Amersham Biosciences) and analyzed using AIDA software (Raytest, Straubenhardt, Germany).

2.14. Statistical analysis

For statistical analysis the software SignaStat(R) version 3.01 from SPSS inc. (Chicago, Illinois, USA) was used. Results were regarded to be statistically different when $P < 0.05$.

3. Results

3.1. Nanoparticle properties

The physico-chemical characteristics of the different nanoparticles in terms of size, polydispersity and zeta potential were determined directly after the preparation, after purification by size exclusion chromatography and after a storage period of about two months at 4 °C.

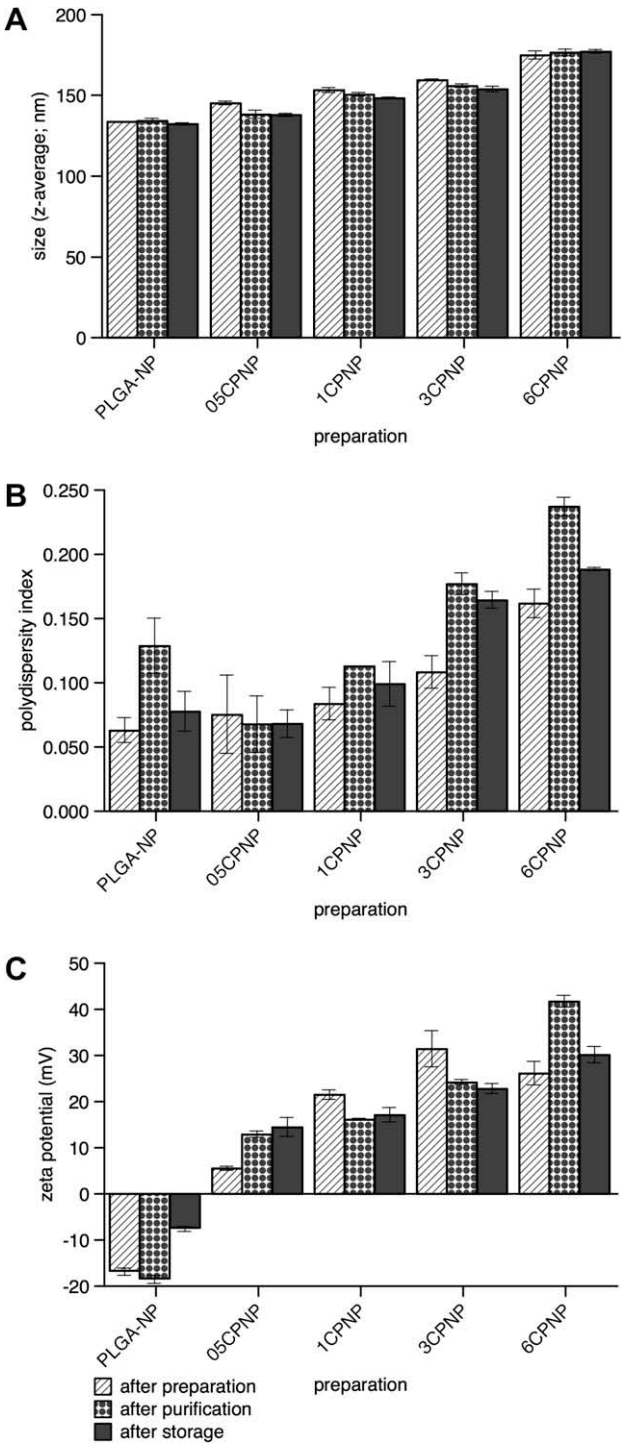

Fig. 1. Properties of different chitosan/PLGA nanoparticles: after preparation (striped bars), after purification (bars with gray circles) and after storage for two months at 4 °C (gray bars); A, size (nm); B, polydispersity index; C, zeta potential (mV). Measurements were performed in triplicate. Data represents mean values ± SD.

As can be seen from Fig. 1A particle sizes were in the range of 135 nm (PLGA-NP) to 175 nm (6CPNP). The increase in size correlated with the amount of chitosan. The purification procedure and storage did not affect the mean particle size for all preparations. In all cases the nanoparticles showed monomodal distribution. However, there was an increase in polydispersity indices (PDIs; Fig. 1B) after purification and storage except for 05CPNP. After preparation PDIs were in the range of 0.060 (PLGA-NP) to 0.160 (6CPNP). After purification they were in the range of 0.070 (05CPNP) to 0.240 (6CPNP) indicating a change in the size distribution because of the purification procedure. This observation is most probably due to a deglomeration of small particle agglomerates. A comparison of the size distribution curves before and after purification revealed that the fraction of smaller particles increased slightly after purification, giving rise to a broadening of the size distribution curves and hence an increase in PDI (data not shown). PDIs decreased again during storage to values below 0.190 (6CPNP). All zeta potentials (ZPs) were positive for preparations containing chitosan while those for PLGA-NP were negative (Fig. 1C). There was a good correlation between chitosan content and increase in zeta potentials after purification. For 05CPNP, 1CPNP and 3CPNP the ZPs remained stable during storage. For 6CPNP there was a drop in ZP from about 42 to 30 mV and PLGA-NP showed an increase from about −19 to −8 mV.

3.2. Complexation of 2OMR

To examine complexation efficiencies and nanoplex stabilities nanoplexes at different 2OMR: nanoparticle w/w ratios were preformed in water and subsequently diluted with either water, PBS or RPMI cell culture medium + 10% FCS. The amounts of unbound 2OMR were determined from the supernatant after removal of nanoplexes by centrifugation.

In MilliQ-water, the amount of unbound 2OMR decreased with increasing amounts of nanoparticles (Fig. 2A). Up to a $w_{2OMR}/w_{particles}$ ratio of 1:25 there was a good correlation between the chitosan content and the binding: particles prepared with higher amount of chitosan bound 2OMR better than particles with lower amounts of chitosan. At higher concentrations of nanoparticles the binding efficiency was between 80% and 100% for all preparations. As expected, there was no binding of oligonucleotides to negatively charged PLGA nanoparticles. For all preparations the pH values decrease gradually with increasing particle concentrations from about pH 5.3 to 3.2 (see insert Fig. 2A).

In PBS the stabilities of preformed nanoplexes proved to be very weak. As can be seen from Fig. 2B there was practically no binding of 2OMR after dilution and incubation of the nanoplexes with PBS for all preparations. pH values remained in the neutral range (pH 7.0–7.4) with increasing amounts of chitosan-coated particles.

A similar result was found in RPMI cell culture medium containing 10% FCS (Fig. 2C). Only at the highest particle concentrations about 10–20% of 2OMR were still bound to the particles. For all preparations pH values remained in the neutral range of 7.4–7.7.

3.3. Uptake of nanoplexes

Cell-associated levels of FAM-labeled 2OMR after incubation with different nanoplex preparations were studied by flow cytometry. Confocal laser scanning microscopy (CLSM) was used to visualize the uptake of nanoplexes (w_{2OMR}/w_{NP} ratio 1:50) and nanoparticles into A549, Calu-3 and hAEpC.

Flow cytometry (Fig. 3A) showed an increase in green fluorescence, i.e. cell-associated 5′-FAM-2OMR levels, which was dependent on the formulation. While the incubation of A549 cells with

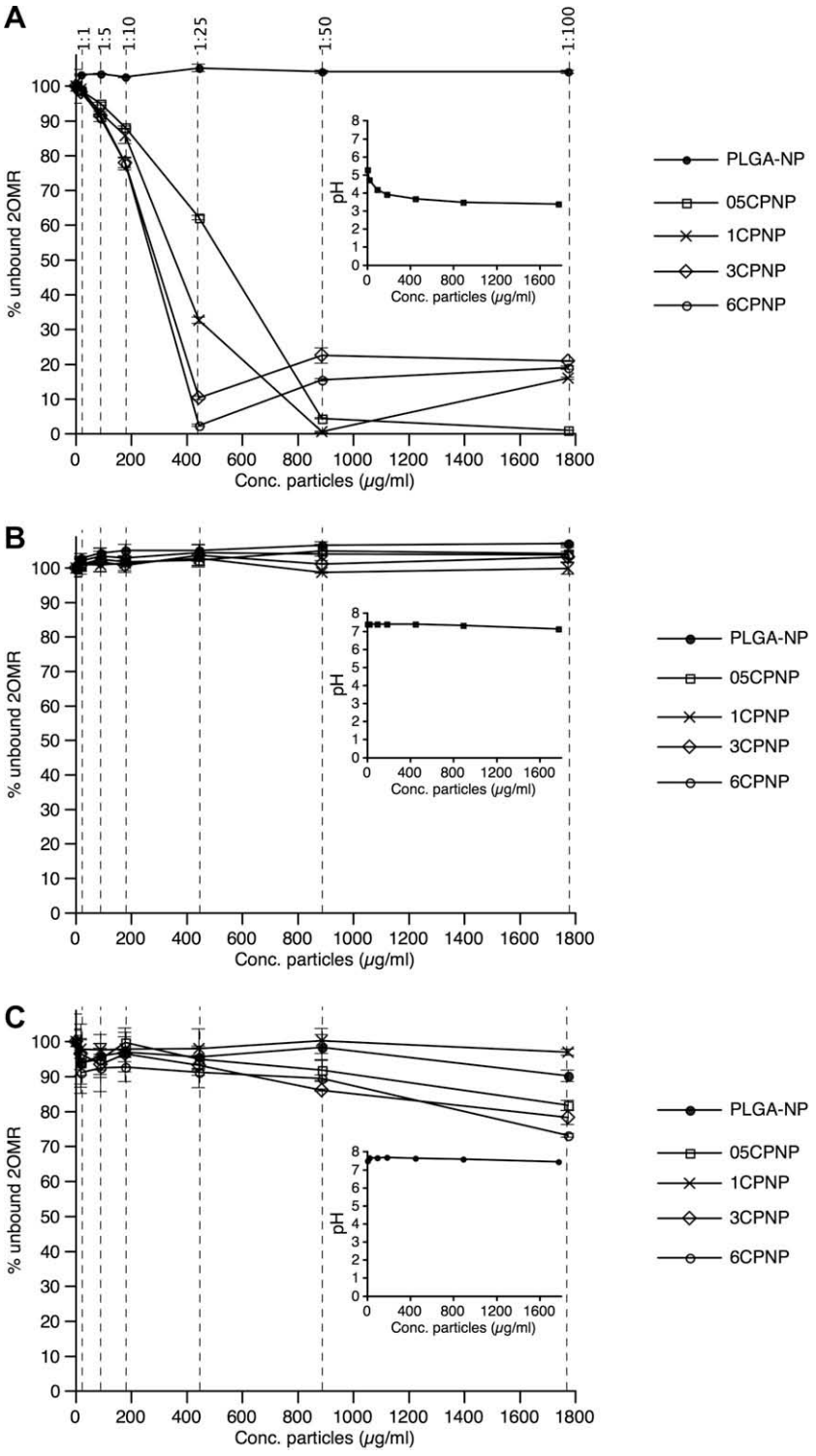

Fig. 2. Binding efficiencies and complex stabilities of nanoplexes between 2OMR and chitosan/PLGA nanoparticles. Nanoplexes were preformed in MilliQ-water and then diluted with: MilliQ-water (A), PBS pH 7.4 (B) and RPMI cell culture medium + 10% FCS (C). The figure shows the percentages of unbound 2OMR recovered from the supernatant after centrifugation referred to the initial amounts. $w_{2OMR}/w_{particles}$ ratios are given on top of the figure and indicated by vertical dashed lines. Inserts: pH profiles for different particle concentrations in respective suspension medium. All experiments were performed in triplicate. Data represents mean values ± SD.

nanoplexes of PLGA-NP did not increase the green fluorescence intensities, there was a shift to higher values with the chitosan-modified PLGA nanoparticles. Best results were obtained for 3CPNP and 6CPNP with about 88% and 83%, respectively. (Fig. 3A). An incubation of cells with plain nanoparticles (i.e. not complexed with 2OMR) showed no interference with this experiment (data not shown). The characterization of the nanoplexes with respect to size and surface charge at the 1:50 ratio (Fig. 3B) demonstrated that nanoplexes prepared with PLGA-NP and 05CPNP were negatively charged. Their sizes were comparable to nanoparticles without 2OMR. 1CPNP exhibited a surface charge around zero mV and the increase in size indicates an agglomeration of the nanoplexes

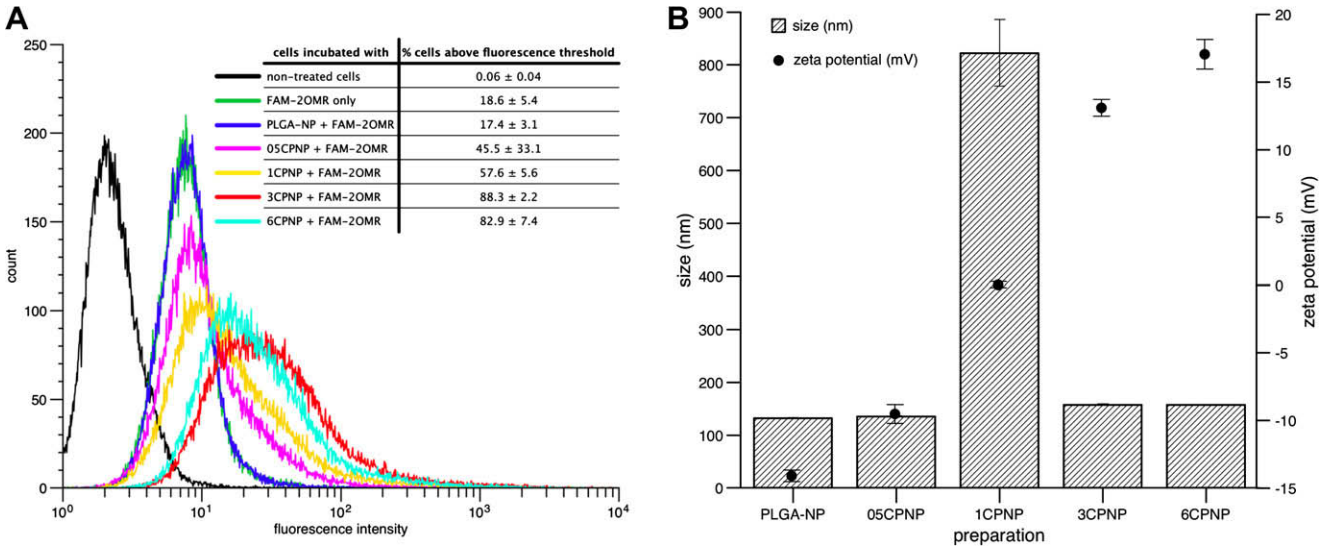

Fig. 3. (A) Histogram from flow cytometry with A549 cells treated with nanoplexes of FAM-labeld 2OMR and different particle preparations at a $w_{2OMR}/w_{particles}$ ratio of 1:50. The green fluorescence of cells was measured 24 h after incubation with nanoplexes. The results in the table were obtained after gating and selection of a fluorescence threshold. 20,000 cells were counted per sample. Values are presented as mean values ± SD ($n = 3$). (B) Properties of nanoplexes at a ratio of 1:50 that were used for flow cytometry experiments measured in MilliQ-water. Bars: size (*z*-average; nm); dots: zeta potential (mV). All measurements were performed in triplicate. Data represents mean values ± SD.

due to the loss of electrostatic repulsion. The sizes of nanoplexes with 3CPNP and 6CPNP were again comparable to the nanoparticles without 2OMR. Both formulations possessed positive surface charges >+10 mV. Since the formulation with 6CPNP did not further increase the cell-associated fluorescence, further experiments were performed with 3CPNP only.

CLSM demonstrated that the increase of fluorescence intensities 24 h after incubation as observed in the flow cytometry experiments is due to an uptake and not only an adsorption of nanoplexes to the cell surface (Fig. 4). As can be seen in Fig. 4 A2–A4 the treatment of A549 cells with nanoplexes of 5′-FAM-2OMR and 3CPNP resulted in a strong green fluorescence compared to cells incubated with 5′-FAM-2OMR alone (Fig. 4A1). Interestingly, the uptake of nanoplexes into A549 cells appeared to be a very slow process. After 6 h of incubation the green fluorescence was still colocalized with the red fluorescence of the cell membranes (Fig. 4A2). An uptake into the cells was observed 24 h post incubation as can be seen in Fig. 4A3. The green fluorescence appeared mostly point-shaped indicating an entrapment of the nanoplexes in intracellular vesicles. A comparable result was obtained 48 h after incubation (Fig. 4A4).

The uptake of nanoplexes into A549 cells was compared to the uptake into Calu-3 cells and non-cancerous hAEpC. In contrast to A549 cells Calu-3 cells also showed an uptake of 5′-FAM-2OMR alone. The green fluorescence intensity and distribution was comparable to cells treated with nanoplexes. Also, there was no adsorption to the cell membrane. The green fluorescence could be observed inside the cells directly after 6 h of incubation (Fig. 4B1 and B2). Comparable to A549 cells the green fluorescence could be observed for at least 48 h (Fig. 4 B3 and B4). In case of non-cancerous hAEpC a colocalization of nanoplexes with the cell membrane was observed but optical sections of these rather thin cells (<1 μm) at least suggested that the nanoplexes were not internalized. The nanoplexes showed a patch-like pattern and where permanently colocalized with the cell membranes for 48 h (Fig. 4 C1–C4).

Nanoplexes prepared of DiI-stained 3CPNP and 5′-FAM-2OMR (Fig. 5) allowed to demonstrate that 2OMR uptake in A549 cells occurred as a complex with the nanoparticles although the complex stability in cell culture medium was very weak (compare Fig. 2C). As can be seen in Fig. 5 the green fluorescence of the oligonucleotides and the red fluorescence of the nanoparticles are colocalized after incubation resulting in a yellowish-orange color. A similar result was obtained 1 and 2 days after incubation indicating a slow release of FAM-2OMR from complexes. However, in comparison to the red fluorescence the green fluorescence seemed to decrease over time. After 5 days red cloudy structures could be found around the cell nuclei (white arrows in Fig. 5). This observation is most probably due to the degradation of the nanoparticles and the release of DiI into the cytoplasm.

3.4. Cytotoxicity and monolayer integrity

The MTT cytotoxicity assay showed that cell survival after a treatment with different concentrations of 3CPNP and nanoplexes of 3CPNP and 2OMR, respectively, is reduced to 70–80% of control independent of nanoparticle concentration (Fig. 6). However, a treatment of cells with a mixture of cell culture medium and water also led to a reduced cell survival (about 90% of control).

Furthermore, the treatment with nanoparticles did not show an effect on monolayer integrity of Calu-3 cells. When grown on Transwell® filters Calu-3 cells typically form tight monolayers with transepithelial electrical resistance (TEER) values between 1300 and 1500 $\Omega \times cm^2$ [11]. TEER for cells incubated with nanoparticles was comparable to controls during the incubation period and 72 h after treatment (data not shown).

3.5. Inhibition of telomerase activity and telomere shortening

The treatment of A549 cells with nanoplexes of either purified (Fig. 7A) or non-purified (Fig. 7B) 3CPNP and 2OMR resulted in comparable reductions of telomerase activity for both batches.

The strongest inhibitory effect was observed after treatment with nanoplexes at a $w_{2OMR}/w_{particles}$ ratio of 1:100 resulting in about 60% inhibition of telomerase activity. However, at this ratio the mismatch control, which contains two mismatches relative to the template sequence [4], also showed a considerable telomerase inhibition. This observation is most probably due to non-specific effects. Best results were obtained with non-purified particles at

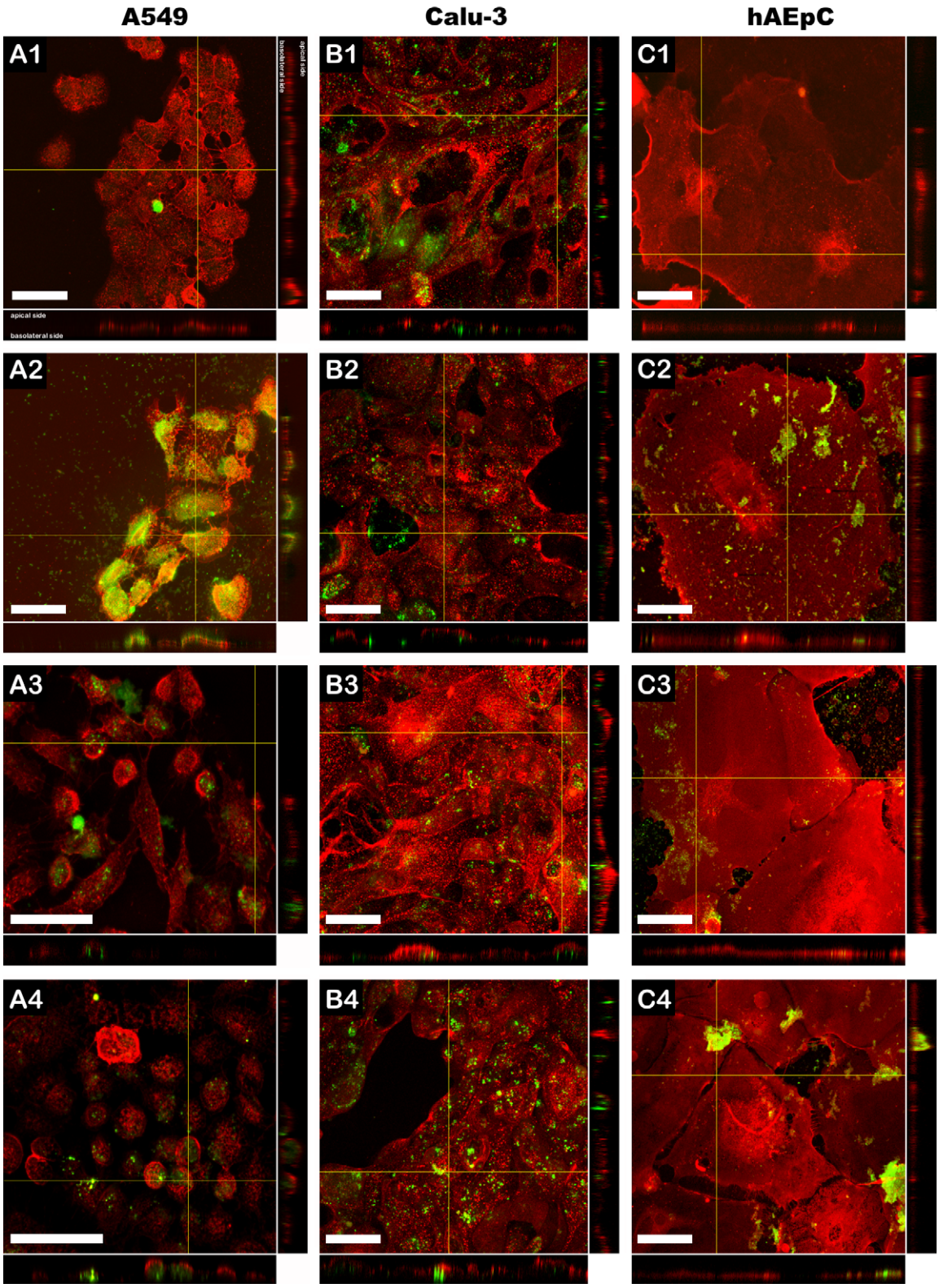

Fig. 4. Confocal images of A549 (A1–A4), Calu-3 (B1–B4) and hAEpC (C1–C4) presented in extended focus mode. Yellow lines indicate the positions of XZ- and YZ-crosssections through image stacks. The location of apical and basolateral sides are given in A1. Bars = 50 μm. A1, B1, C1: cells after 6 h of incubation with 4 μM of FAM-2OMR only; A2, B2, C2: cells after 6 h of incubation with nanoplexes of FAM-2OMR and 3CPNP ($w_{2OMR}/w_{particles}$ ratio: 1:50); A3, B3, C3: cells 24 h after incubation; A4, B4, C4: cells 48 h after incubation. Green fluorescence, FAM-labeled 2OMR; red fluorescence, cell membranes counterstained with Rho-RRCA. FAM-2OMR alone is not taken up into A549 cells and hAEpC (A1 and C1) but into Calu-3 cells (B1). A549: after 6 h of incubation nanoplexes of FAM-2OMR and 3CPNP are colocalized with the cell membrane (A2) but can be found inside the cells after 24 and 48 h (A3 and A4). Calu-3: nanoplexes are directly taken up after 6 h of incubation (B2). hAEpC: The green fluorescence is colocalized with the cell membrane for 48 h (C2–C4).

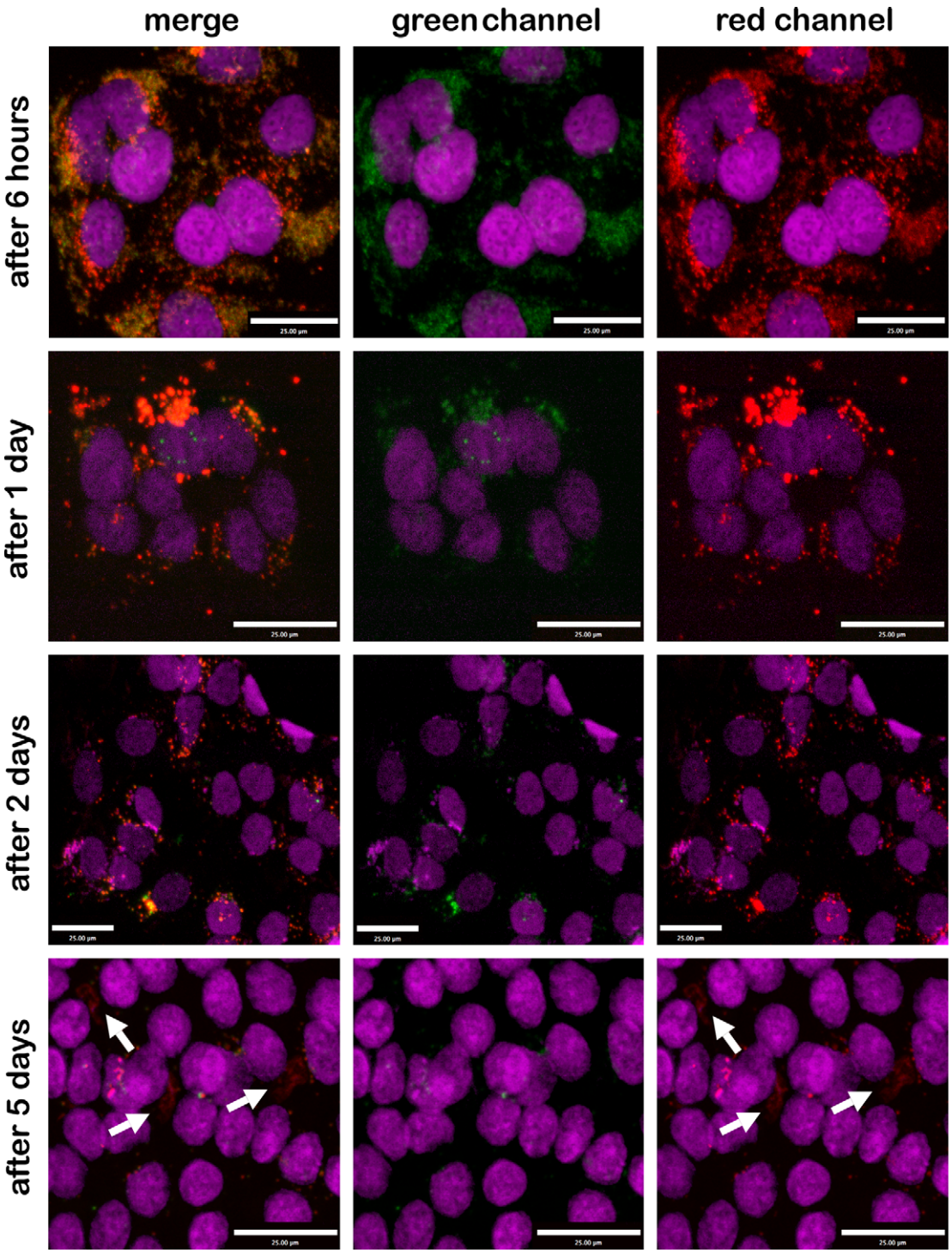

Fig. 5. The uptake of 2OMR in A549 cells is mediated via nanoplexes. The green fluorescence of FAM-2OMR is colocalized with the red fluorescence from DiI-stained 3CPNP. Colocalization can be observed for at least two days by the yellowish/orange color in the left column ("merge"). Middle column and right column: fluorescence of FAM-2OMR (green) and DiI-3CPNP (red), respectively. After five days red cloudy structures (white arrows) indicate the degradation of nanoparticles and release of DiI into the cytoplasm. Purple, cell nuclei counterstained with TOPRO-3. Bars, 25 µm.

the 1:50 ratio. Here, a statistically significant difference between normal 2OMR and the mismatch sequence has been found ($P < 0.05$). Telomerase activity was decreased by about 50% with normal 2OMR while mismatch 2OMR showed only a slight effect. Such a statistically significant difference between normal and mismatch 2OMR could not be found for purified particles. The telomerase inhibition by nanoplexes prepared with non-purified nanoparticels was as efficient as using the lipid-based transfection reagents DOTAP and MegaFectin™, which was described recently by our group Beisner et al. [12].

Reduction of telomere length was examined after repetitive treatments (twice weekly) of A549 cells over 35 days in compari-

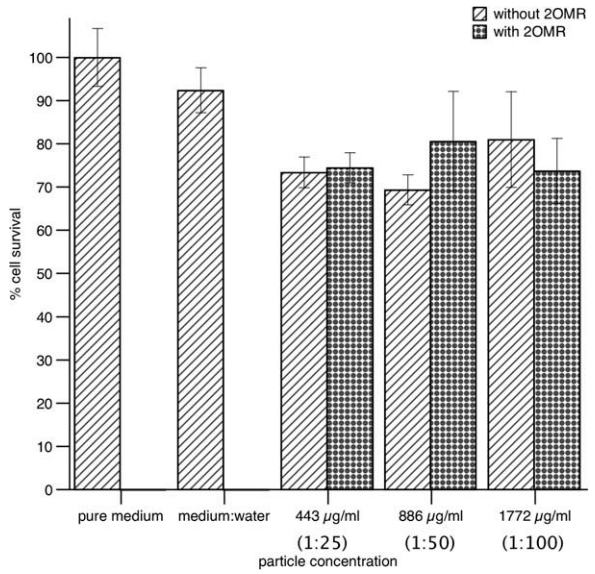

Fig. 6. MTT assay with purified 3CPNP: A549 cells show a reduced survival in the presence of nanoparticles and nanoplexes. Cells were treated with nanoplexes of the $w_{2OMR}/w_{particles}$ ratios 1:25 (=443 µg/ml nanoparticles), 1:50 (=886 µg/ml nanoparticles) and 1:100 (=1772 µg/ml nanoparticles). Cells treated only with plain nanoparticles in the corresponding concentrations were used as controls. Each concentration was measured in quadruplicate. Data represents mean values ± SD.

son with the lipid-based transfection reagents DOTAP and Mega-Fectin™. As can be seen in Fig. 8, 3CPNP were as effective as the two commercial transfection reagents. Reduction in telomere length was significant for all three preparations compared to control ($P < 0.05$; One-way-ANOVA) but there was no significant difference between the transfection reagents.

4. Discussion

Our results show that changing the amounts of chitosan in the preparation procedure can easily vary particle properties. These variations significantly influence their efficiency for the delivery of antisense 2OMR to lung cancer cells.

The particles proved to be stable after purification and storage over two months and they showed a high binding of 2OMR and complex stability in water. However, dilution in buffered media strongly reduced complex formation. In our previous study, suspensions of CPNP either as particles alone or in complex with 2OMR proved to be stable in NaCl solution, PBS, pH 7.4, and HBSS buffer, pH 7.4, with regard to their colloidal properties. However, they showed a strong reduction in their surface charge when diluted in buffered media, which is due to the neutralization of the protonated primary amine groups of chitosan [8]. This charge neutralization results in a reduced ability to bind the negatively charged 2OMR as could be demonstrated by our binding/complexation experiments. Chitosan is a weak base. The type that was used for these experiments has a pK_a value of about 6.5 [13]. Complexes diluted in pure MilliQ-water were stable because pH values were below this pK_a resulting in protonation of most of the amino groups. In contrast, due to the neutralization of the positive charges, complex stability was strongly reduced and dissociation occurred when the preformed complexes were diluted in buffered media like PBS and cell culture medium with pH values $\geqslant 7$.

From these results one could expect that nanoplexes in cell culture medium are unstable and do not improve the uptake of 2OMR into cells. But this was not the case. As we could demonstrate in the following experiments with A549 cells, uptake was significantly increased for nanoplexes prepared with 3CPNP and 6CPNP and telomerase was activity successfully inhibited (Figs. 3–5, 7 and 8).

From the nanoplex characterizations it could be argued that the uptake correlated with the particle surface charge (Fig. 3B) as described by Lorenz et al. [14]. However, the characterization was performed in water while the uptake experiments were performed in cell culture medium containing 10% fetal calf serum. Beside the neutralization of the surface charge in cell culture medium it is known that serum proteins adsorb to cationic nanoparticles [15,16], which significantly influences the surface charge. The fact that there was no difference in uptake improvement between nanoplexes prepared with 3CPNP and 6CPNP indicates that the uptake cannot only be attributed to the surface charge but also must be related to the chitosan density on the particle surface. That the uptake of FAM-2OMR into A549 is really mediated via nanoplexes could clearly be demonstrated by confocal microscopy (Figs. 4 and 5), which shows that that there is no complete dissociation of com-

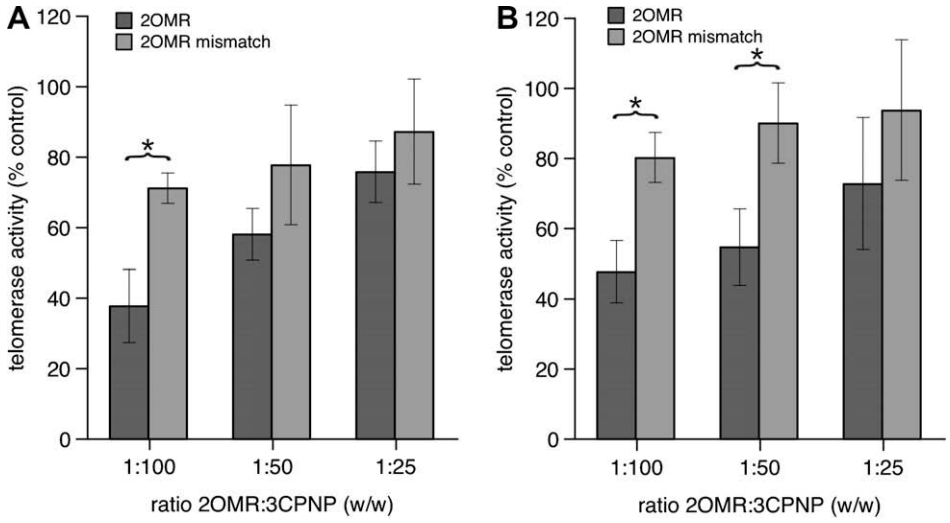

Fig. 7. Reduction of telomerase activities in A549 cells 72 h after incubation with 2OMR:3CPNP nanoplexes at different w/w ratios in comparison to a 2OMR mismatch control. Telomerase activities were normalized to non-treated cells. (A) nanoplexes were formed with purified 3CPNP nanoparticles; (B) nanoplexes were formed with non-purified 3CPNP nanoparticels. Data represent mean values ± SD of at least 3 independent experiments. *, statistically significant difference between normal 2OMR and mismatch control ($P < 0.05$, One-way ANOVA).

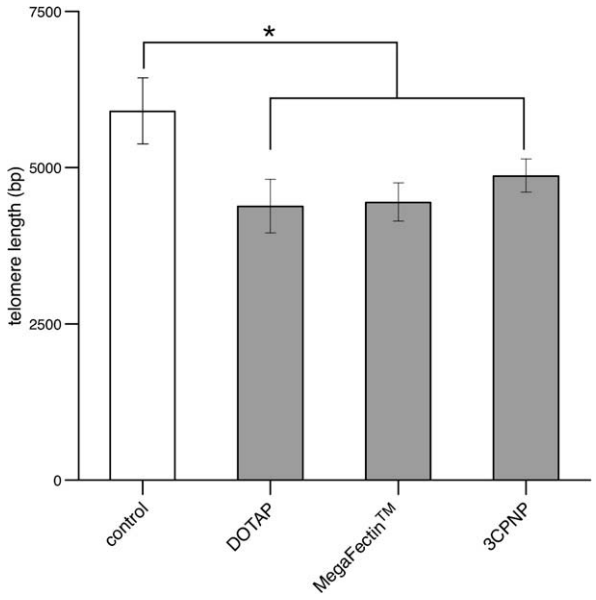

Fig. 8. Telomere length in A549 cells after repeated treatment with 2OMR:3CPNP nanoplexes over 35 days in comparison to cells treated with the commercially available transfection reagents DOTAP and MegaFectin™. 3CPNP are as efficient as DOTAP and MegaFectin™. *, all treated cells were statistically significant different from control (One-way-ANOVA; $P < 0.05$). There was no statistical significant difference between the lipid-based transfection reagents and 3CPNP.

plexes in cell culture medium and that the nanoplexes are still able to interact with the cell surface. Whether these non-dissociated complexes corresponds to the about 15% of bound 2OMR (Fig. 2C; 1:50 ratio 3CPNP) will be the subject of future studies. Fang et al. have shown with liposomes composed of DPPC that even at pH 7.4, an adhesion between chitosan and the phospholipid membrane occurs [17]. Löhbach et al. demonstrated that the adhesion of chitosan-coated carboxypolystyrene nanoparticles dispersed in PBS to endothelial cells is higher in the presence of FCS than without proteins [18]. Therefore, besides remaining ionic forces other factors like hydrogen bonds or even the combination of chitosan and proteins on the particle surfaces might play an important role in the nanoplex–cell surface interaction.

Huang et al. reported that the uptake of FITC-labeled chitosan nanoparticles into A549 cells is a saturable process dependent on adsorption of particles to the cell membrane and subsequent clathrin-mediated endocytosis [19,20]. This mechanism corresponded well to the observations in our experiments. The uptake of FAM-2OMR alone was very poor but the adsorption of nanoplexes to the cell surface significantly enhanced its internalization. The results from flow cytometry suggest that a certain chitosan density on the particle surface is required to achieve optimal adsorption. This level was reached in 3CPNP because 6CPNP with their higher chitosan content did not further increase the nanoplex uptake (Fig. 3A). The differences in chitosan content were shown by zeta potential measurements in this (Figs. 1 and 3B) and our previous study [8] where 6CPNP exhibit a higher zeta potential than 3CPNP.

However, nanoplexes also adsorbed on hAEpCs, but no clear internalization was observed over two days. HAEpC are primary isolated human alveolar type (AT) II cells that acquire characteristics of AT I cells after a certain time under the given cell culture conditions [21]. Since AT I cells are reported to be deficient in clathrin-mediated endocytosis [22] this might explain the lack of nanoplex internalization by these cells. In contrast, Calu-3 expressing both clathrin and caveolin [23] showed even an uptake of FAM-2OMR alone. However, a closer investigation of the exact uptake mechanism was not done.

The data from the MTT toxicity test demonstrates that the nanoparticles have only a slight cytotoxicity as they reduce the A549 cell growth about 20–30% (Fig. 6). The nanoparticles did not influence the integrity of Calu-3 monolayers, and hence their barrier function, since TEER values did not differ from controls. Grenha et al. reported a comparable result for chitosan nanoparticles in respirable powder formulations [24].

Furthermore, we were able to show that a treatment of A549 cells with these nanoplexes results in an inhibition of telomerase activity and telomere shortening. The comparison of our chitosan/PLGA nanoparticles with established transfection reagents was encouraging for further studies since the results were comparable to DOTAP or MegaFectin™. However, the purification of CPNP does not seem to be necessary with regard to their biological effect because telomerase inhibition was not significantly different for either purified or non-purified particles. Regarding the specificity of 2OMR in comparison with the mismatch sequence, nanoplexes prepared with non-purified particles appeared to be even more effective than those prepared with purified particles. For this study purification was done to assure that the observed effects in binding and uptake experiments can only be attributed to the nanoparticles and not to remaining polymers in the suspensions. Since the presence of these polymers does not seem to influence the biological activity future studies concerning the long-term efficacy of nanoplexes will be performed with non-purified particles.

5. Conclusion

Nanoplexes formed between cationic chitosan-coated PLGA nanoparticels and antisense 2′-*O*-methyl-RNA were efficiently taken up by human alveolar (A549) and bronchial (Calu-3) epithelial cancer cell lines, while cellular uptake was not obvious for non-cancerous human alveolar epithelial cells in primary culture. In thus transfected cells, a significant inhibition of telomerase activity and shortening of telomeres could be observed. Transfection proved to be dependent on the chitosan content if the nanoplexes, allowing to optimize the formulation for such application. The resulting nanoplexes were well tolerated by the cells and appeared to be equally efficient as some commercially available lipid-based transfection reagents.

Acknowledgements

This project is financially supported by Deutsche Krebshilfe e.V. (Project No.: 10-2035-Kl I) and the Robert Bosch Foundation (Stuttgart, Germany).

References

[1] E.H. Blackburn, Telomeres and telomerase: their mechanisms of action and the effects of altering their functions, FEBS Lett. 579 (2005) 859–862.
[2] J.W. Shay, W.E. Wright, Senescence and immortalization: role of telomeres and telomerase, Carcinogenesis 26 (2004) 867–874.
[3] K. Piotrowska, E. Kleideiter, T.E. Mürdter, S. Taetz, C. Baldes, U.F. Schaefer, C.M. Lehr, U. Klotz, Optimization of the TRAP assay to evaluate specificity of telomerase inhibitors, Lab. Invest. 85 (2005) 1565–1569.
[4] A.E. Pitts, D.R. Corey, Inhibition of human telomerase by 2′-*O*-methyl-RNA, Proc. Natl. Acad. Sci. USA 95 (1998) 11549–11554.
[5] B. Herbert, A.E. Pitts, S.I. Baker, S.E. Hamilton, W.E. Wright, J.W. Shay, D.R. Corey, Inhibition of human telomerase in immortal human cells leads to progressive telomere shortening and cell death, Proc. Natl. Acad. Sci. USA 96 (1999) 14276–14281.
[6] M.N. Ravi Kumar, U. Bakowsky, C.M. Lehr, Preparation and characterization of cationic PLGA nanospheres as DNA carriers, Biomaterials 25 (2004) 1771–1777.
[7] M.N. Ravi Kumar, S.S. Mohapatra, X. Kong, P.K. Jena, U. Bakowsky, C.M. Lehr, Cationic poly(lactide-co-glycolide) nanoparticles as efficient in vivo gene transfection agents, J. Nanosci. Nanotechnol. 4 (2005) 990–994.
[8] N. Nafee, S. Taetz, M. Schneider, U.F. Schaefer, C.M. Lehr, Chitosan-coated PLGA nanoparticles for DNA/RNA delivery: effect of the formulation parameters on

complexation and transfection of antisense oligonucleotides, Nanomedicine 3 (2007) 173–183.
[9] K.J. Elbert, U.F. Schafer, H.J. Schafers, K.J. Kim, V.H. Lee, C.M. Lehr, Monolayers of human alveolar epithelial cells in primary culture for pulmonary absorption and transport studies, Pharm. Res. 16 (1999) 601–608.
[10] C. Ehrhardt, K.J. Kim, C.M. Lehr, Isolation and culture of human alveolar epithelial cells, Methods Mol. Med. 107 (2005) 207–216.
[11] N.R. Mathias, J. Timoszyk, P. Stetsko, J. Megill, R. Smith, D. Wall, Permeability characteristics of Calu-3 human bronchial epithelial cells: in vitro–in vitro correlation to predict lung absorption in rats, J. Drug Target. 10 (2002) 31–40.
[12] J. Beisner, M. Dong, S. Taetz, K. Piotrowska, E. Kledeideiter, G. Friedel, U.F. Schaefer, C.-M. Lehr, U. Klotz, T.E. Mürdter, Efficient telomerase inhibition in human non-small cell lung cancer cells by liposomal delivery of 2-O-methyl-RNA, J. Pharm. Sci. (2008), in press.
[13] P. Sorlier, A. Denuzière, C. Viton, A. Domard, Relation between the degree of acetylation and the electrostatic properties of chitin and chitosan, Biomacromolecules 2 (2001) 765–772.
[14] M.R. Lorenz, V. Holzapfel, A. Musyanovych, K. Nothelfer, P. Walther, H. Frank, K. Landfester, H. Schrezenmeier, V. Mailänder, Uptake of functionalized, fluorescent-labeled polymeric particles in different cell lines and stem cells, Biomaterials 27 (2006) 2820–2828.
[15] A. Gessner, A. Lieske, B. Paulke, R. Müller, Influence of surface charge density on protein adsorption on polymeric nanoparticles: analysis by two-dimensional electrophoresis, Eur. J. Pharm. Biopharm. 54 (2002) 165–170.
[16] M. Lück, B.R. Paulke, W. Schröder, T. Blunk, R.H. Müller, Analysis of plasma protein adsorption on polymeric nanoparticles with different surface characteristics, J. Biomed. Mater. Res. 39 (1998) 478–485.
[17] N. Fang, V. Chan, Interaction of liposome with immobilized chitosan during main phase transition, Biomacromolecules 4 (2003) 581–588.
[18] C. Löhbach, D. Neumann, C.M. Lehr, A. Lamprecht, Human vascular endothelial cells in primary cell culture for the evaluation of nanoparticle bioadhesion, J. Nanosci. Nanotechnol. 6 (2006) 1–7.
[19] M. Huang, Z. Ma, E. Khor, L.Y. Lim, Uptake of FITC-chitosan nanoparticles by A549 cells, Pharm. Res. 19 (2002) 1488–1494.
[20] M. Huang, E. Khor, L.Y. Lim, Uptake and cytotoxicity of chitosan molecules and nanoparticles: effects of molecular weight and degree of deacetylation, Pharm. Res. 21 (2004) 344–353.
[21] S. Fuchs, A.J. Hollins, M. Laue, U.F. Schaefer, K. Roemer, M. Gumbleton, C.M. Lehr, Differentiation of human alveolar epithelial cells in primary culture: morphological characterization and synthesis of caveolin-1 and surfactant protein-C, Cell Tissue Res. 311 (2003) 31–45.
[22] M. Gumbleton, Caveolae as potential macromolecule trafficking compartments within alveolar epithelium, Adv. Drug Deliv. Rev. 49 (2001) 281–300.
[23] N.A. Bradbury, J.A. Clark, S.C. Watkins, C.C. Widnell, H.S. Smith, R.J. Bridges, Characterization of the internalization pathways for the cystic fibrosis transmembrane conductance regulator, Am. J. Physiol. 276 (1999) L659–L668.
[24] A. Grenha, C.I. Grainger, L.A. Dailey, B. Seijo, G.P. Martin, C. Remuñán-López, B. Forbes, Chitosan nanoparticles are compatible with respiratory epithelial cells in vitro, Eur. J. Pharm. Sci. (2007).